**EMITTER International Journal of Engineering Technology**
Vol. 12, No. 2, December 2024, pp. 182~195
DOI : 10.24003/emitter.v12i2.890

# Development of Differential Optical Absorption Spectroscopy (DOAS) System for Hazardous Methane Gas Detection in the Near Infrared Region

**Sayma Khandaker, Md Mahmudul Hasan, Nurulain Shaipuzaman, Mohd Amir Shahlan Mohd Aspar, Hadi Manap**

Faculty of Electrical and Electronics Engineering Technology, Universiti Malaysia Pahang Al-Sultan Abdullah, Pekan, Pahang, Malaysia
Corresponding Author: hadi@umpsa.edu.my

*Received September 28, 2024; Revised November 5, 2024; Accepted December 7, 2024*

**Abstract**

Methane ($CH_4$) is a powerful greenhouse gas that greatly contributes to global warming. It is also very combustible, which means it has a large danger of causing explosions. It is crucial to tackle methane emissions, especially those arising from oil and gas extraction processes like transit pipes. An area of great potential is the advancement of dependable sensors for the detection and reduction of methane leaks, with the aim of averting dangerous consequences. An open-path differential optical absorption spectroscopy (DOAS) system was described in this paper for the purpose of detecting $CH_4$ gas emission at a moderate temperature. An in-depth examination of the absorption lines was conducted to determine the optimal wavelength for measurement. The Near Infrared (NIR) region was identified as the most suitable wavelength for detecting methane. Multiple measurements were conducted at different integration times (1 second, 2 seconds, and 3 seconds) to ensure reliability and determine the optimal integration time for the $CH_4$ detection system. The DOAS system has the capability of precisely detecting methane concentrations at 1M ppm in the NIR region with a quick integration time of 2 seconds.

**Keywords**: Methane detection, DOAS technique, Optical sensor, NIR region

## 1. INTRODUCTION

Methane ($CH_4$), a major constituent of hydrocarbons, is an exceedingly potent greenhouse gas (GHG). The global temperature potential of this substance is considerably greater than that of carbon dioxide, particularly when considering shorter time frames [1]. The energy sector is responsible for a quarter of all methane emissions in the U.S. known as fugitive emissions [2, 3]. Minimizing the release of methane is crucial, particularly if we want to depend on natural gas for electric power in order to maintain the stability of future energy systems that heavily rely on unpredictable renewable sources.

Industrialization has led to a substantial rise in the amount of methane in the environment. In 2016, the level of methane reached as high as 1800 parts per billion (ppb), compared to around 800 ppb at the start of the 19th century [4]. The main anthropogenic sources of emissions causing this increase include garbage disposal facilities, livestock waste disposal systems, coal extraction, petrochemical exploration, electrical transformers, and gas and oil transportation and production facilities [5]. Moreover, in the event that the level of methane gas in a confined space above 5 to 15%, it has the potential for combustion and result in a fire [6]. Due to its ample availability and comparatively secure burning method, natural gas is anticipated to be widely employed in the future, although its adverse effects on the environment remain unknown [7]. As reported by the World Health Organization (WHO), $CH_4$ has an aggregate atmospheric lifespan of 12 years until it is gradually eliminated by chemicals like OH radicals. This constitutes a serious ecological risk when released into the air [8, 9].

Several recent studies [10–14] have discovered $CH_4$ emissions that exceed the projections provided by the Environmental Protection Agency (EPA) in its GHG emission assessment. Indeed, the EPA has increased the assumptions for methane emissions in its most recent survey [15]. Current research efforts have enhanced our knowledge of $CH_4$ emissions from different parts of the fossil fuel supply chain, including extraction [10, 11, 16], treatment [17], transfer [18], and distribution [14, 19]. However, it is challenging to determine and measure the specific sources of human-caused emissions due to the wide range and geographical spread of possible leaking. Furthermore, numerous local research conducted using aircraft have consistently discovered emission rates that deviate from the anticipated emission levels [10, 20]. Approximately 64% of $CH_4$ emissions originate from anthropogenic sources, such as rubbish dumps, paddy cultivation, farming, and livestock decomposition [21, 22], as shown in Figure 1.

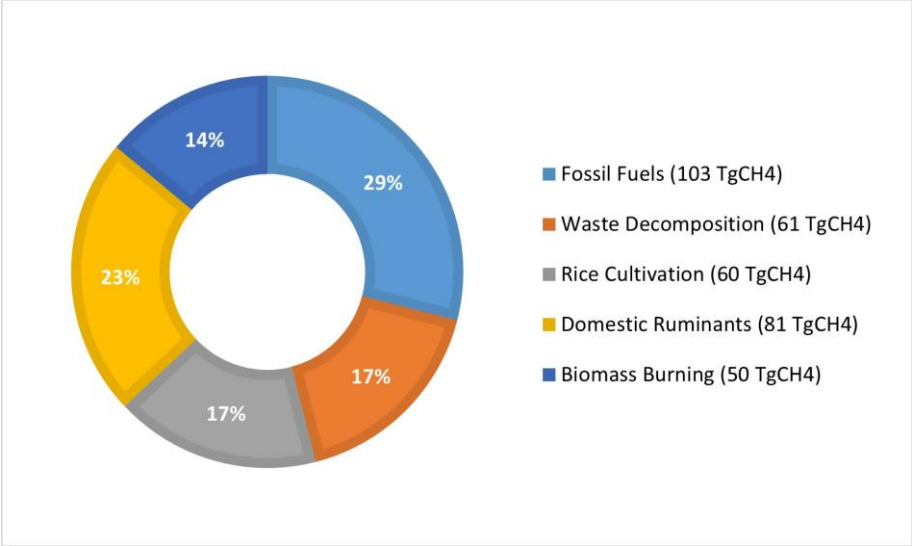


**Figure 1.** Individual sources of the total emissions of methane around the world

This research presents an open-path optical approach for methane detection. The term commonly used to describe this method is differential optical absorption spectroscopy (DOAS). The primary benefit of utilizing a DOAS technique is its capacity to identify many gas types in immediate time [23–25]. This occurs due to the DOAS system often permits a concurrent line of absorb reaction linked to numerous molecules of greenhouse gasses. Initially, the DOAS system is primarily committed to identifying signs of methane gas throughout its initial phases of advancement. Emphasizing the recognition of a single gas in its infancy is crucial to guarantee the highest accuracy, sensitivity, and reliability of the sensor system before conducting testing for several greenhouse gases in the future.

### 1.1. What is DOAS?

The DOAS technique utilizes a Deuterium-Halogen light source to identify methane. Nevertheless, methane gas may be identified utilizing the identical optical absorption method in the infrared band.

DOAS is a highly utilized approach for quantifying the levels of minor gases present in the surrounding air. DOAS concept entails the examination of the absorption of both visible and ultraviolet light by gases in the air [26]. Light, emitted by a source such as the sun, synthetic light, or light scattered from the sky, propagates throughout the environment. When light travels through the atmosphere, different gases take light at particular wavelengths, resulting in a distinct absorption spectrum for every gas.

Once the light has interacted with the gas in the atmosphere around it, it is then gathered by a spectrometer. The spectrometer separates the light into its constituent wavelengths, allowing for thorough study. The essence of DOAS resides in the comparative analysis of absorbing characteristics. The instrument quantifies the absorption characteristics that are overlaid on a wide, gradually changes in background. This enables it to separate the absorption caused by small amounts of gases from other influences like scattering and overall absorption.

The DOAS technique is highly efficient in identifying and measuring small amounts of gases and contaminants [27]. The extreme specificity and sensitivity of this technology make it highly important for conducting environmental studies, observing the natural world, and assessing the air's cleanliness. DOAS may precisely identify and quantify different air components through contrasting the obtained absorption spectra with reference spectra of known gases. This technique plays a crucial role in gathering vital information for comprehending and addressing pollution.

## 2. RELATED WORKS

$CH_4$ is a powerful GHG with a global temperature potential of 86 times that of carbon dioxide during a 20-year period, and significantly greater for shorter time periods [28]. Lowering methane emissions and implementing methane reduction strategies may effectively mitigate global warming in the

short run. Multiple types of sensors, such as visual, pyroelectric, semiconducting metal oxide, electrolytic, and calorimetric sensors, are capable of identifying methane [29].

Recently, infrared methane identification equipment has been growing in prominence because of its various benefits, such as extended lifespan, strong dependability, broad usefulness, and reliable identification abilities [30]. A methane detector equipped with an optical correlator provides enhanced choice by precisely corresponding gas absorption lines [31]. Tunable diode laser absorption Spectroscopy is an adaptable and effective optical method for detecting gases [32]. This approach allows for the execution of the measurements, whether they are done in person or remotely. Dong et al., [33] introduced a cavity boosted technique for methane identification. This method involved systematically varying the length of the cavity while scanning the laser frequency to accurately measure the propagation peaks of the cavity phases. An inexpensive and compact diode-laser absorption spectroscope with configurable infrared capabilities, utilizing silicon-based chip-scale photonics integration, designed specifically for methane sensors [34]. The researchers utilized an uncooled InGaAs recognition approach combined with an extremely sensitive silicon waveguide at the nanoscale to assess atmospheric methane. They used near-IR (1650 nm) light from a laser with dispersed feedback. As a result, they achieved a limit of identification below 100 ppm-v. Furthermore, there has been a recent advancement in using UAVs that are directed from a distance to identify methane. This presents a viable method for identifying leaks of natural gas in pipelines [28, 35].

To summarize, there are signs of considerable advancement in enhancing the efficacy of the various methane techniques and sensors that were mentioned. However, it is important to note that these techniques still possess some functional limitations. The drawbacks of these systems include expensive implementation in large-scale environments and limited selectivity caused by the absence of clear differentiation in the methane optical absorption range. One additional drawback of these methods is that they necessitate ongoing human supervision.

## 3. ORIGINALITY

The second dominant greenhouse gas produced by humans, methane ($CH_4$), has a major impact on warming the planet. Therefore, it is imperative to decrease emissions of methane in order to mitigate the rise in temperatures caused by human-induced greenhouse gases. A crucial component of any plan aimed at reducing methane emissions is the capacity to precisely recognize and track the quantity and distribution of methane produced by different sectors. The contributions of the present investigation are presented as follows:

- To the best of authors knowledge, this is the first study to detect hazardous methane gas utilizing DOAS technique.

- The most suitable wavelength region for $CH_4$ gas detection is investigated.
- The study is carried out within various integration time (1 second, 2 seconds, and 3 seconds) to determine the optimal integration time to detect $CH_4$.

## 4. SYSTEM DESIGN

### 4.1 Theory

Various gas types exhibit distinct light absorption patterns at certain wavelengths, and methane gas possesses a unique gas absorption spectrum. The Max Planck Institute provides a thorough compilation of absorption cross-sections for gaseous molecules, which can be obtained through the MPI-Mainz UV-VIS database [36]. This set comprises information regarding methane gas as well.

The statistics obtained from this collection [36] exhibit variations between different sources and are contingent upon heat and the variety of wavelengths. Just a single factor that aligns with the hypothesis is chosen and then compared. According to the analysis of the absorption cross-section in [29], methane gas has the ability to take in light at various wavelengths within the NIR region.

Based on the optical studies, the interaction between the light with the material or experimental sample can be visualized through Beer's Lambert Law equation. Equation (1) represents the Beer-Lambert equation, which explains the direct correlation between the absorbance and concentration of a substance that absorbs light.

$$\frac{I}{I_0} = e^{(-\sigma.N.l)} \tag{1}$$

Where $I$ represent the intensity of the light that is carried, $I_0$ represent the strength of the incoming light, and $l$ (cm) represent the length of time that light passes across gas, $N$ (molecules/cm$^3$) is the gas concentration and $\sigma$ (cm$^2$/molecule) is the absorption cross-section.

Equation (1) is created to determine the absorption cross section, whereas Equation (2) provides a modified version of the Beer-Lambert Law. The specifics of the deduction were previously documented in a prior publication [37].

$$\sigma = \frac{-[ln\frac{I}{I_0}][24.4]}{ppm \times N_A \times I \times 10^{-9}} \tag{2}$$

### 4.2 Unit Conversion

In Equation (1) of the Beer-Lambert Law, the concentration of the testing gas *N*, is given as Molecules/cm$^3$. Converting to ppm is essential for precise concentration measurements of harmful gases because that is the industry standard.

The ideal gas law (PV = nRT) is also employed in this unit change, where *P* = pressure (atm), *V* = volume (L), *n* = mass of substance (moles), *R* = ideal gas constant (0.082 atm L mol$^{-1}$K$^{-1}$), *T* = absolute temperature ($^0$C + 273) in degrees Kelvin.

$$\frac{V}{n} = \frac{RT}{P} = \frac{(0.082 \frac{atm\ .\ L}{mol\ .\ K})(273K)}{1\ atm} = 22.4\ \frac{L}{mol} \tag{3}$$

The standard temperature and pressure are 0$^0$C (273 K) and 1 atm, respectively. A mole of the ideal gas covers a volume of 22.4 L according to these circumstances.

Occasionally, gaseous quantities are expressed as the ratio of mass to volume, denoted as mg/m$^3$. The correlation of mg/m$^3$ and ppm is mainly affected by the gas's bulk density, that is regulated by its temperature, molecular weight, and pressure. This is illustrated in Equation (4).

$$\rho\left(\frac{mg}{m^3}\right) = \frac{ppm \times \omega}{22.4 \frac{L}{mol}} \times \frac{273}{T\ (K)} \times \frac{P\ (atm)}{1\ atm} \tag{4}$$

Where *T*(K) is the recorded temperature, $\rho$(mg/m$^3$) is the gas density, *P*(atm) is the quantified pressure, and $\omega$ is the molecular weight of the test gas.

Equation (4) is frequently employed and can be streamlined as demonstrated in Equation (5), assuming that the temperature of the test gas is 298 K and the pressure is 1 atm.

$$\rho\left(\frac{mg}{m^3}\right) = \frac{ppm \times \omega}{22.4 \frac{L}{mol}} \tag{5}$$

In order to utilize Equation (5) and determine the amount in ppm units, it is necessary to establish the relationship involving the gas density, $\rho$ (mg/m$^3$), and the concentration of the test gas, *N* (Molecules/cm$^3$).

Since *N*(Molecules/cm$^3$) * (1000 mg/1g) * (1 cm$^3$/10$^{-6}$m$^3$) * (1 mol/6.022x10$^{23}$ Molecules) * $\omega$ (g/mol) = $\rho$(mg/m$^3$). Therefore, the relationship between $\rho$(mg/m$^3$) and *N*(Molecules/cm$^3$) is depicted in Equation (6).

$$N = \frac{\rho}{\omega}\ N_A \times\ 10^{-9} \tag{6}$$

Where $N_A$ is the Avogadro's constant.

To determine the gas concentration, N in ppm, we substitute Equations (5) and (6) into the Beer-Lambert Law Equation (1). Therefore,

$$ppm = \frac{-\left[\ln \frac{I}{I_0}\right][24.4]}{\sigma \times N_A \times l \times 10^{-9}} \quad (7)$$

By utilizing Equation (7), we can precisely determine the gas concentration when $\sigma$ has been determined. The value of $\sigma$ fluctuates based on the observed wavelength.

Conceptual gas concentrations provide a robust basis for comparing with actual concentrations obtained from the sensor. They are commonly used during the creation phase of new sensing techniques. To determine the theoretical gas concentrations, it is necessary to have knowledge of the rate at which gases flow throughout the testing phases.

### 4.3 Experimental Setup

The test was conducted at the Faculty of Electrical and Electronics Engineering Technology, Universiti Malaysia Pahang Al-Sultan Abdullah. Figure 2 displays the experimental setup. The light source used in the test was a Deuterium-Halogen lamp, specifically the DH-2000 model manufactured by Ocean Optics. The light was propagated through a UVNS fiber (Ultraviolet Non-Solarizing) manufactured by CeramOptec Inc., with a core size of 644.4 nm. Two collimating lenses were positioned at opposite extremities of the gas cell to concentrate incoming and outgoing light. Subsequently, the light that was sent proceeded through a separate optical cable located at the opposite end of the gas cell being tested, ultimately reaching the light detector. The light detector utilized in this research was an Ocean Optics HR2000 spectrometer. The spectrometer has a wavelength region of 200 nm to 1200 nm, which is capable of resolving features with a precision of 0.65 nm (FWHM). The spectrometer was linked to a computer through the use of SpectraSuite software. SpectraSuite is a specialized software developed by Ocean Optics for the purpose of collecting current information from the spectrometer. The intensity of the light that was sent, $I$, and the intensity of the incident light, $I_0$, were measured, and Equation (6) was utilized to measure the absorption cross section. The outcome was graphed in relation to the wavelength and then compared to the theoretical predictions.

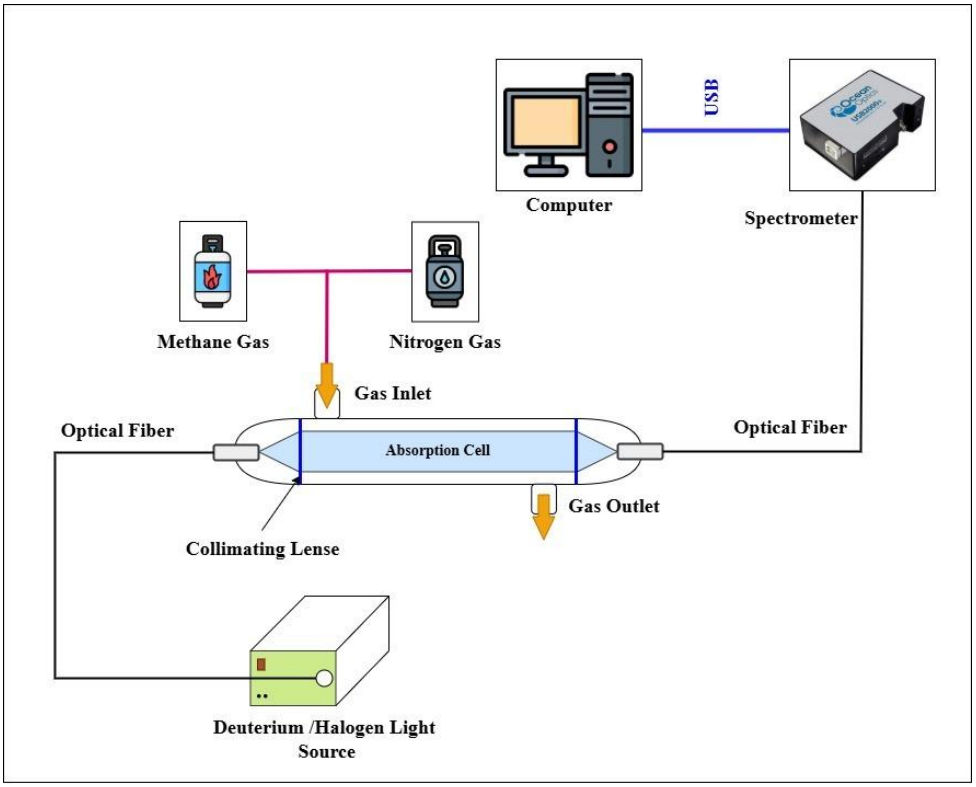


**Figure 2.** Laboratory experimental setup

## 5. EXPERIMENT AND ANALYSIS

At first, nitrogen ($N_2$) gas was discharged in the test gas container. When $N_2$ gas was introduced into the test gas cell, it had no effect on the methane measurement. Because $N_2$ gas is inert and non-reactive under most conditions, which means it does not participate in chemical reactions with the analytes (gases being measured) or the optical components [38]. Using $N_2$ as an inert gas in DOAS helps to ensure accurate, repeatable, and interference-free measurements, which is critical for detecting trace gases in environmental monitoring, industrial emissions, and other applications.

Multiple measurements were conducted at varying integration times (1 second, 2 seconds, and 3 seconds) to ensure significance and determine the optimal integration time for the $CH_4$ detection system. An integration time of 2 seconds was selected as the most suitable, as it outperformed the other durations.

Figure 3 illustrates the absorption cross-section of $CH_4$ in the 870-920 nm range, confirming that the presence of $N_2$ gas does not interfere with the analysis. The absorption peaks of $CH_4$ are clearly observed within this wavelength range, which falls in the NIR region, indicating successful detection using DOAS. The results confirm that the measurement system is robust against the presence of $N_2$ gas, ensuring reliable detection of $CH_4$ under these conditions.

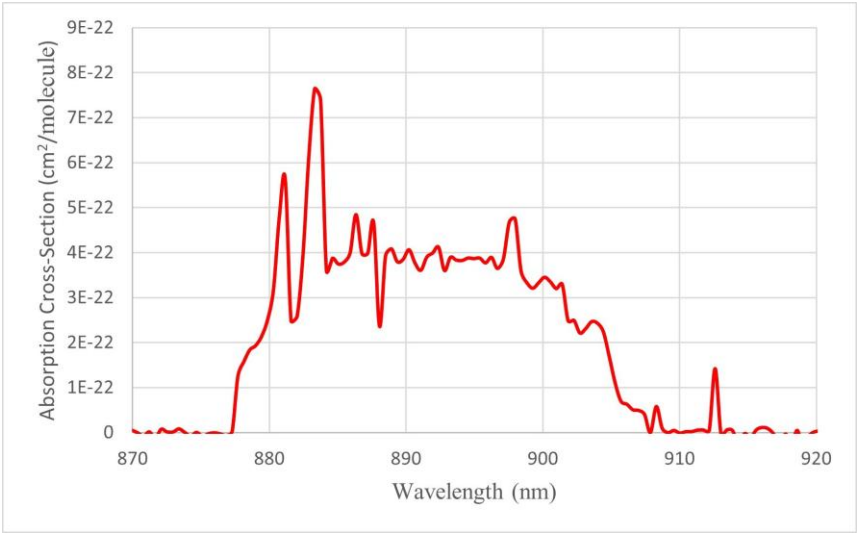


**Figure 3.** Methane absorption cross section in NIR region for 2 second integration time

To confirm and validate $CH_4$ detection using the DOAS system, the experimental results were compared with theoretical data. Figure 4 shows a comparison between the theoretical and experimental $CH_4$ absorption cross-sections. While the measured $CH_4$ spectrum generally aligns with the theoretical pattern, notable discrepancies are present, particularly in the lower wavelength region. These discrepancies can be attributed to a significant reduction in signal strength, likely caused by the optical fiber at shorter wavelengths.

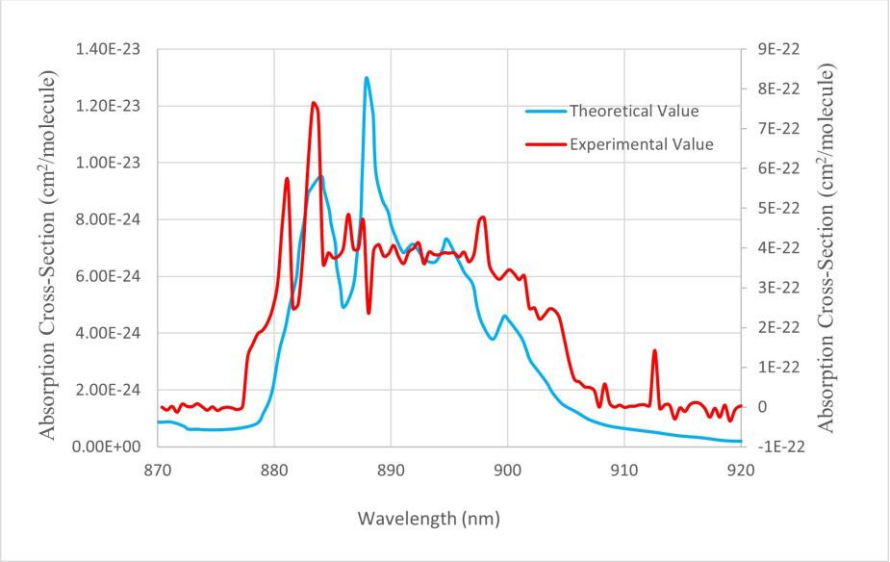


**Figure 4.** Methane absorption cross-section spectrum comparison between theoretical data and experimental data

Theoretical data from the MPI database [36] indicates that $CH_4$ absorption occurs within the 870–920 nm wavelength range in the NIR region. Similarly, the experimental measurements of this study investigated a closely aligned range of 870–920 nm, within the NIR region.

However, the experimental absorption patterns are similar, the experimental values are shifted approximately 4 nm to the left. This shift is likely attributed to an inaccurate calibration of the spectrometer. Another possible explanation for the shift could be environmental factors, such as stray light or the instrument's slit entrance, affecting the measurements. Besides, the theoretical data were obtained using intracavity laser spectroscopy (ILS), while the experimental data were acquired through the DOAS technique. The methodological differences between ILS and DOAS likely account for the structural variations between the two spectra. Nonetheless, despite these differences, the measured wavelength range for methane detection closely matches the theoretical values and falls within the NIR region, further confirming the accuracy and reliability of the DOAS system for $CH_4$ detection.

## 6. CONCLUSION

An innovative optical fiber-based DOAS technique for detecting $CH_4$ gas is presented. The results demonstrate that this method is effective in identifying methane absorption within the NIR wavelength region. Additionally, the measured $CH_4$ data depicts a pattern closely resembling the spectrum obtained from the MPI Mainz database. Thus, utilizing the NIR band to detect $CH_4$ concentrations proves to be a promising approach. Future research will focus on conducting comprehensive in-situ experimental tests to further analyze and optimize the performance of the sensing system for practical applications.

## Acknowledgments

The authors would like to express their sincere gratitude to the Universiti Malaysia Pahang Al-Sultan Abdullah (UMPSA) for their support and provision of research funds for this project (PDU233203). Additionally, the authors would like to express their sincere gratitude to the Faculty of Electrical and Electronics Engineering Technology, Universiti Malaysia Pahang Al-Sultan Abdullah (UMPSA) for providing access to a few facilities.

## REFERENCES

[1] A. P. Ravikumar, J. Wang, and A. R. Brandt, **Are Optical Gas Imaging Technologies Effective For Methane Leak Detection?**, *Environ. Sci. Technol.*, vol. 51, no. 1, pp. 718–724, Jan. 2017, doi: 10.1021/acs.est.6b03906.

[2] A. R. Brandt et al., **Methane Leaks from North American Natural Gas Systems**, *Science*, vol. 343, no. 6172, pp. 733–735, Feb. 2014, doi: 10.1126/science.1247045.

[3] D. R. Lyon, R. A. Alvarez, D. Zavala-Araiza, A. R. Brandt, R. B. Jackson, and S. P. Hamburg, **Aerial Surveys of Elevated Hydrocarbon Emissions from Oil and Gas Production Sites**, *Environ. Sci. Technol.*, vol. 50, no. 9, pp. 4877–4886, May 2016, doi: 10.1021/acs.est.6b00705.

[4] A. J. Turner, C. Frankenberg, and E. A. Kort, **Interpreting contemporary trends in atmospheric methane**, *Proc. Natl. Acad. Sci. U.S.A.*, vol. 116, no. 8, pp. 2805–2813, Feb. 2019, doi: 10.1073/pnas.1814297116.

[5] **About Methane Emissions**, *Government of Canada*, 2014. [Online]. Available: https://www.canada.ca/en/environment-climate-change/services/climate-change/global-methane-initiative/about-methane-emissions.html

[6] Intergovernmental Panel On Climate Change, Ed., **Climate Change 2013 – The Physical Science Basis: Working Group I Contribution to the Fifth Assessment Report of the Intergovernmental Panel on Climate Change**, *1st ed. Cambridge University Press*, 2014. doi: 10.1017/CBO9781107415324.

[7] M.-K. Tran and M. Fowler, **A Review of Lithium-Ion Battery Fault Diagnostic Algorithms: Current Progress and Future Challenges**, *Algorithms*, vol. 13, no. 3, p. 62, Mar. 2020, doi: 10.3390/a13030062.

[8] A. M. Thompson, K. B. Hogan, and J. S. Hoffman, **Methane reductions: Implications for global warming and atmospheric chemical change**, *Atmospheric Environment*. Part A. General Topics, vol. 26, no. 14, pp. 2665–2668, Oct. 1992, doi: 10.1016/0960-1686(92)90118-5.

[9] N. Lawrence, **Analytical detection methodologies for methane and related hydrocarbons**, *Talanta*, vol. 69, no. 2, pp. 385–392, Apr. 2006, doi: 10.1016/j.talanta.2005.10.005.

[10] A. Karion et al., **Aircraft-Based Estimate of Total Methane Emissions from the Barnett Shale Region**, *Environ. Sci. Technol.*, vol. 49, no. 13, pp. 8124–8131, Jul. 2015, doi: 10.1021/acs.est.5b00217.

[11] T. N. Lavoie et al., **Aircraft-Based Measurements of Point Source Methane Emissions in the Barnett Shale Basin**, *Environ. Sci. Technol.*, vol. 49, no. 13, pp. 7904–7913, Jul. 2015, doi: 10.1021/acs.est.5b00410.

[12] D. R. Lyon et al., **Constructing a Spatially Resolved Methane Emission Inventory for the Barnett Shale Region**, *Environ. Sci. Technol.*, vol. 49, no. 13, pp. 8147–8157, Jul. 2015, doi: 10.1021/es506359c.

[13] X. Lan, R. Talbot, P. Laine, and A. Torres, **Characterizing Fugitive Methane Emissions in the Barnett Shale Area Using a Mobile Laboratory**, *Environ. Sci. Technol.*, vol. 49, no. 13, pp. 8139–8146, Jul. 2015, doi: 10.1021/es5063055.

[14] K. McKain et al., **Methane emissions from natural gas infrastructure and use in the urban region of Boston, Massachusetts**, *Proc. Natl. Acad. Sci. U.S.A.*, vol. 112, no. 7, pp. 1941–1946, Feb. 2015, doi: 10.1073/pnas.1416261112.

[15] **Inventory of U.S. Greenhouse Gas Emissions and Sinks: 1990-2014**, *US Environmental Protection Agency*, 2016. [Online]. Available: https://www.epa.gov/ghgemissions/inventory-us-greenhouse-gas-emissions-and-sinks-1990-2014

[16] M. Omara, M. R. Sullivan, X. Li, R. Subramanian, A. L. Robinson, and A. A. Presto, **Methane Emissions from Conventional and Unconventional Natural Gas Production Sites in the Marcellus Shale Basin**, *Environ. Sci. Technol.*, vol. 50, no. 4, pp. 2099–2107, Feb. 2016, doi: 10.1021/acs.est.5b05503.

[17] A. J. Marchese et al., **Methane Emissions from United States Natural Gas Gathering and Processing**, *Environ. Sci. Technol.*, vol. 49, no. 17, pp. 10718–10727, Sep. 2015, doi: 10.1021/acs.est.5b02275.

[18] D. J. Zimmerle et al., **Methane Emissions from the Natural Gas Transmission and Storage System in the United States**, *Environ. Sci. Technol.*, vol. 49, no. 15, pp. 9374–9383, Aug. 2015, doi: 10.1021/acs.est.5b01669.

[19] B. K. Lamb et al., **Direct Measurements Show Decreasing Methane Emissions from Natural Gas Local Distribution Systems in the United States**, *Environ. Sci. Technol.*, vol. 49, no. 8, pp. 5161–5169, Apr. 2015, doi: 10.1021/es505116p.

[20] J. Peischl et al., **Quantifying atmospheric methane emissions from oil and natural gas production in the Bakken shale region of North Dakota**, *JGR Atmospheres*, vol. 121, no. 10, pp. 6101–6111, May 2016, doi: 10.1002/2015JD024631.

[21] R. B. Jackson et al., **Increasing anthropogenic methane emissions arise equally from agricultural and fossil fuel sources**, *Environ. Res. Lett.*, vol. 15, no. 7, p. 071002, Jul. 2020, doi: 10.1088/1748-9326/ab9ed2.

[22] J. Kamieniak, E. P. Randviir, and C. E. Banks, **The latest developments in the analytical sensing of methane**, *TrAC Trends in Analytical Chemistry*, vol. 73, pp. 146–157, Nov. 2015, doi: 10.1016/j.trac.2015.04.030.

[23] H. Manap and M. S. Najib, **A DOAS system for monitoring of ammonia emission in the agricultural sector**, *Sensors and Actuators B: Chemical*, vol. 205, pp. 411–415, Dec. 2014, doi: 10.1016/j.snb.2014.08.080.

[24] G. Dooly, H. Manap, S. O'Keeffe, and E. Lewis, **Highly Selective Optical Fibre Ammonia Sensor for use in Agriculture**, *Procedia Engineering*, vol. 25, pp. 1113–1116, 2011, doi: 10.1016/j.proeng.2011.12.274.

[25] S. O'Keeffe, H. Manap, G. Dooly, and E. Lewis, **Real-time monitoring of agricultural ammonia emissions based on optical fibre sensing technology**, *in 2010 IEEE Sensors*, Kona, HI: IEEE, Nov. 2010, pp. 1140–1143. doi: 10.1109/ICSENS.2010.5690821.

[26] **Differential Optical Absorption Spectroscopy**, *Physics of Earth and Space Environments*. Berlin, Heidelberg: Springer Berlin Heidelberg, 2008. doi: 10.1007/978-3-540-75776-4.

[27] Q. Gao, W. Weng, B. Li, M. Aldén, and Z. Li, **Gas Temperature Measurement Using Differential Optical Absorption Spectroscopy (DOAS)**, *Appl Spectrosc*, vol. 72, no. 7, pp. 1014–1020, Jul. 2018, doi: 10.1177/0003702818760864.

[28] D. Hollenbeck, D. Zulevic, and Y. Chen, **Advanced Leak Detection and Quantification of Methane Emissions Using sUAS**, *Drones*, vol. 5, no. 4, p. 117, Oct. 2021, doi: 10.3390/drones5040117.

[29] T. Aldhafeeri, M.-K. Tran, R. Vrolyk, M. Pope, and M. Fowler, **A Review of Methane Gas Detection Sensors: Recent Developments and Future Perspectives**, *Inventions*, vol. 5, no. 3, p. 28, Jul. 2020, doi: 10.3390/inventions5030028.

[30] X. Yu, R.-H. Lv, F. Song, C.-T. Zheng, and Y.-D. Wang, **Pocket-Sized Nondispersive Infrared Methane Detection Device Using Two-Parameter Temperature Compensation**, *Spectroscopy Letters*, vol. 47, no. 1, pp. 30–37, Jan. 2014, doi: 10.1080/00387010.2013.780082.

[31] L. Polerecky, C. S. Burke, and B. D. MacCraith, **Optimization of absorption-based optical chemical sensors that employ a single-reflection configuration**, *Appl. Opt.*, vol. 41, no. 15, p. 2879, May 2002, doi: 10.1364/AO.41.002879.

[32] J. B. McManus, **Application of quantum cascade lasers to high-precision atmospheric trace gas measurements**, *Opt. Eng*, vol. 49, no. 11, p. 111124, Nov. 2010, doi: 10.1117/1.3498782.

[33] L. Dong, W. Yin, W. Ma, L. Zhang, and S. Jia, **High-sensitivity, large dynamic range, auto-calibration methane optical sensor using a short confocal Fabry–Perot cavity**, *Sensors and Actuators B: Chemical*, vol. 127, no. 2, pp. 350–357, Nov. 2007, doi: 10.1016/j.snb.2007.04.030.

[34] L. Tombez, E. J. Zhang, J. S. Orcutt, S. Kamlapurkar, and W. M. J. Green, **Methane absorption spectroscopy on a silicon photonic chip**, *Optica*, vol. 4, no. 11, p. 1322, Nov. 2017, doi: 10.1364/OPTICA.4.001322.

[35] S. Iwaszenko, P. Kalisz, M. Słota, and A. Rudzki, **Detection of Natural Gas Leakages Using a Laser-Based Methane Sensor and UAV**, *Remote Sensing*, vol. 13, no. 3, p. 510, Jan. 2021, doi: 10.3390/rs13030510.

[36] **MPI-Mainz-UV-VIS Spectral Atlas of Gaseous Molecules**. Accessed: Apr. 13, 2024. [Online]. Available: http://www.atmosphere.mpg.de/enid/2295

[37] H. Manap, G. Dooly, S. O'Keeffe, and E. Lewis, **Ammonia detection in the UV region using an optical fiber sensor**, *in 2009 IEEE Sensors*, Christchurch, New Zealand: IEEE, Oct. 2009, pp. 140–145. doi: 10.1109/ICSENS.2009.5398215.

[38] M. Mitu, M. Prodan, V. Giurcan, D. Razus, and D. Oancea, **Influence of inert gas addition on propagation indices of methane–air deflagrations**, *Process Safety and Environmental Protection*, vol. 102, pp. 513–522, Jul. 2016, doi: 10.1016/j.psep.2016.05.007.